available at www.sciencedirect.com

ScienceDirect

journal homepage: www.elsevier.com/locate/biochempharm

Growth inhibitory activity of cucurbitacin glucosides isolated from *Citrullus colocynthis* on human breast cancer cells

Tehila Tannin-Spitz [a], *Shlomo Grossman* [a,*], *Sara Dovrat* [a], *Hugo E. Gottlieb* [b], *Margalit Bergman* [a]

[a] *The Mina & Everard Goodman Faculty of Life Sciences, Bar-Ilan University, Ramat-Gan 52900, Israel*
[b] *Department of Chemistry, Bar-Ilan University, Ramat-Gan 52900, Israel*

ARTICLE INFO

Article history:
Received 11 July 2006
Accepted 11 September 2006

Keywords:
Apoptosis
Breast cancer
Cucurbitacin glucoside
F-actin
G_2/M
$p34^{CDC2}$

Abbreviations:
ER, estrogen receptor
FACS, fluorescence activated cell sorting
FCS, foetal calf serum
JC-1, 5,5′,6,6′-tetrachloro-1,1′,3,3′-tetraethyl-benzamidazolocarbocyanin iodide
MTT, 3-(4,5-dimethylthiazol-2-yl)-2,5-diphenyl tetrazolium bromide
NMR, nuclear magnetic resonance
PI, propidium iodide
TLC, thin layer chromatography

ABSTRACT

Our aim was to study the effects of cucurbitacin glucosides extracted from *Citrullus colocynthis* leaves on human breast cancer cell growth. Leaves were extracted, resulting in the identification of cucurbitacin B/E glucosides. The cucurbitacin glucoside combination (1:1) inhibited growth of ER^+ MCF-7 and ER^- MDA-MB-231 human breast cancer cell lines. Cell-cycle analysis showed that treatment with isolated cucurbitacin glucoside combination resulted in accumulation of cells at the G_2/M phase of the cell cycle. Treated cells showed rapid reduction in the level of the key protein complex necessary to the regulation of G_2 exit and initiation of mitosis, namely the $p34^{CDC2}$/cyclin B1 complex. cucurbitacin glucoside treatment also caused changes in the overall cell morphology from an elongated form to a round-shaped cell, which indicates that cucurbitacin treatment caused impairment of actin filament organization. This profound morphological change might also influence intracellular signaling by molecules such as PKB, resulting in inhibition in the transmission of survival signals. Reduction in PKB phosphorylation and inhibition of survivin, an anti-apoptosis family member, was observed. The treatment caused elevation in p-STAT3 and in $p21^{WAF}$, proven to be a STAT3 positive target in absence of survival signals. Cucurbitacin glucoside treatment also induced apoptosis, as measured by Annexin V/propidium iodide staining and by changes in mitochondrial membrane potential ($\Delta\Psi$) using a fluorescent dye, JC-1. We suggest that cucurbitacin glucosides exhibit pleiotropic effects on cells, causing both cell cycle arrest and apoptosis. These results suggest that cucurbitacin glucosides might have therapeutic value against breast cancer cells.

* *Corresponding author*. Tel.: +972 3 5318050; fax: +972 3 6356869/5351824.
E-mail address: grossms@mail.biu.ac.il (S. Grossman).
0006-2952/$ – see front matter © 2006 Elsevier Inc. All rights reserved.
doi:10.1016/j.bcp.2006.09.012

1. Introduction

Breast cancer affects one in every 10 women in Western Europe and the USA [1], and it is the second leading cause of cancer-related deaths [2]. Treatments include surgery, radiation, and in some cases, drugs that are specifically targeted such as herceptin, in the case of tumors that overexpress EGF receptor, or tamoxifen, in the case of estrogen-dependent tumors [3]. However, the majority of cases, especially those that result in metastasis, are still treated with conventional chemotherapy. The problem of drug resistance is a major obstacle in chemotherapeutic treatment, therefore, there is a great need for the development of new therapeutic drugs that will be more efficient or will synergize with the existing ones.

There has been a growing interest in the use of herbs as a potent source of new therapeutic anticancer drugs. Plants contain a wide variety of chemicals that have potent biological effects, including anticancer activity [4]. Recently, we presented the mechanism of NAO (natural antioxidants) from spinach and derived purified components [5,6] acting through G1 arrest [7]. Moreover, we reviewed the efficacy of these natural compounds in various biological systems [8–10]. In this research, we focused on the antiproliferative effect of the cucurbitacin glucosides isolated from *Citrullus colocynthis*.

C. colocynthis (L.) Shrad (Cucurbitaceae), locally known as Sherry or Handal, is used in folk medicine by people in rural areas as a purgative, antirheumatic, and as a remedy for skin infections. The plant contains cucurbitacins A, B, C, and D, α-elaterin, and probably other constituents [11].

The cucurbitacins (highly oxygenated tetracyclic triterpens) are of great interest because of the wide range of biological activity they exhibit in plants and animals. They are predominantly found in the cucurbitaceae family but are also present in several other families of the plant kingdom. Species of the plants in which they are found have been used for centuries in various pharmacopoeia. A number of compounds of this group have been investigated for their cytotoxic, hepatoprotective, anti-inflammatory, cardiovascular effects and anti-diabetic effects [12]. Several studies were published pointing out that different cucurbitacin species exhibit various biological activities against tumor expansion. For instance, cucurbitacin I and Q were shown to specifically inhibit STAT3 phosphorylation, which contributes to the proliferation of many cancerous cells [13,14]. Another study reported that cucurbitacin E inhibits the proliferation of prostate cancer cells and causes disruption of the cytoskeleton structure of actin and vimentin [15,16]. Cucurbitacin B, D, E, and I inhibited the growth of several cancer cell lines and inhibited COX-2 enzyme rather than COX-1 [12]. Cucurbitacin B was shown to exhibit anti-inflammatory activity [17,18].

The purpose of the present study was to examine the effects of the cucurbitacin glucosides (B and E) extracted from *C. colocynthis* on human breast cancer cells, including the effects on cellular growth, cell-cycle distribution, apoptosis, and the expression of proteins involved in cell-cycle regulation, utilizing both estrogen-dependent (MCF-7) and estrogen-independent (MDA-MB-231) human breast cancer cell lines.

To this end, we succeeded in isolating and describing by nuclear magnetic resonance (NMR) analysis the molecular structure of both cucurbitacin B and E glucosides. We also explored the mechanism by which they reduce the proliferation of human breast cancer cells and found that cucurbitacin B and E glucosides can cause accumulation of cells in the G_2/M phase of the cell cycle accompanied with induction of apoptosis. In addition, we looked into the signaling mechanism by which the cucurbitacin glucosides exert their beneficial effects in the chemoprevention of breast cancer cells.

2. Material and methods

2.1. Extraction and isolation procedures

Leaves of *C. colocynthis* (L.) Shrad (collected from an open field at Bar-Ilan University) were mixed 1:4 (w/v) with distilled water and homogenized. The homogenate was filtered, centrifuged and the supernatant was dried in a lyophilizer (0.07 mbar, −48 °C). The powder was further extracted in 70% chloroform/methanol, filtered, and evaporated under reduced pressure. The resulting extract was tested by thin-layer chromatography (TLC) (silica gel 60 F_{254} plates, Merck Eurolab SA, France) using the solvent system: chloroform/methanol (9:1). The fraction with $R_f = 0.56$ was a mixture of two cucurbitacin B and E glucosides (1:1). By further TLC using benzene–ethanol (8:2), we succeeded in separating between the cucurbitacin glucosides.

2.2. Identification of molecular structure by NMR

NMR spectra of the cucurbitacin glucosides were obtained on a Bruker DMX-600 spectrometer, at 600.1 MHz (^{1}H) and 150.9 MHz (^{13}C), respectively, at room temperature. The solvent used was a mixture of 10% CD_3OD and 90% $CDCl_3$, containing 0.1% TMS as internal reference. NMR analysis was facilitated by the use of 2D experiments such as COSY (^{1}H × ^{1}H correlation), HMQC (one-bond ^{13}C × ^{1}H correlation), and HMBC (long-range ^{13}C × ^{1}H correlation).

2.3. Cell culture

MCF-7 (ER positive) and MDA-MB-231 (ER negative) were obtained from the American type culture collection (Rockville, MD, USA). Cells were grown in RPMI-1640 medium (Biological Industries Inc., Kibbutz Beit Haemek, Israel) supplemented with 10% (v/v) foetal calf serum (FCS), 1% penicillin–streptomycin–nystatin. Cells were maintained at 37 °C in a humidified atmosphere of 5% CO_2 in air.

2.4. Cell proliferation and viability assay

The effect of the cucurbitacin glucoside treatment on proliferation of MCF-7 and MDA-MB-231 cells was measured by 3-(4,5-dimethylthiazol-2-yl)-2,5-diphenyl tetrazolium bromide (MTT) (Sigma, MO, USA) assay based on the ability of live cells to cleave the tetrazolium ring to a molecule that absorb at 570 nm [19]. 7×10^3 cells were grown on a 96-well microliter plate and incubated with cucurbitacin B/E glucoside or their combination (4, 8, and 20 μM) in RPMI-10% FCS medium. After 24, 48, and 72 h, the medium was changed and 130 μl/well of fresh RPMI-1640 media was added. Next, 20 μl MTT reagent

(5 mg/1 ml PBS) was added to each well, and the cells were further incubated at 37 °C for 2 h. To determine lysis of the cells, 100 μl N,N-dimethyl formamid solution (50% final concentration of N,N-dimethyl formamid and 20% of sodium dodecyl sulphate, pH 4.7) was added to each well for an additional 7 h, followed by reading on a scanning multiwell spectrophotometer.

2.5. Flow cytometry

MCF-7 and MDA-MB-231 cells (5×10^5) were seeded in 100-mm culture dishes, and allowed to attach overnight. The medium was replaced with fresh complete medium containing the desired concentration of cucurbitacin B/E glucoside (B: 20 and 33 μM; E: 15 and 25 μM) or their combination (8 and 20 μM). Cells were incubated for 24 h at 37 °C. The cells were washed with PBS and then spun at 300 × *g*. The pellet was resuspended in 250 μl PBS and 250 μl propidium iodide (PI) (50 μg/ml final concentration) for 15 min, and analyzed using a flow cytometer.

2.6. Western blot analysis

MCF-7 and MDA-MB-231 cells (1×10^6) were seeded in 100-mm culture dishes. The cells were treated with the cucurbitacin glucoside combination (20 μM) in RPMI-1640 media for 1, 4 or 24 h. The media was then aspirated, and cells were washed with cold PBS. The cells were scraped and washed twice by centrifugation at 500 × *g* for 5 min at 4 °C. The pellet was resuspended in lysis buffer supplemented with proteases and phosphotase inhibitors and incubated for 1 h at 4 °C. The lysate was collected by centrifugation at 14,000 × *g* for 40 min at 4 °C, and the supernatant (total cell lysate) was stored at −20 °C. For Western blot analysis, 40 μg protein was resolved over 12% polyacrylamide gels and transferred to a nitrocellulose membrane. The blot was blocked in blocking buffer (1% non-fat dry milk/1% Tween 20 in PBS) for 1 h at room temperature, incubated with appropriate monoclonal primary antibodies (human reactive anti-$p34^{CDC2}$, anti-Survivin, anti-STAT3 from Santa Cruz Biotechnology, anti-Cyclin B1 from Biosource, and anti-$p21^{WAF}$ from BD Biosciences) or polyclonal primary antibodies (human reactive anti-phospho-$p34^{CDC2}$ (Thr14 and Tyr15) from Santa Cruz, anti-phospho-STAT3 (Tyr 705), anti-AKT, and anti-phospho-AKT (Ser 473) from cell signaling) in blocking buffer overnight at 4 °C. The blot was then incubated with appropriate secondary antibody horseradish peroxidase conjugate and detected by chemiluminescence and autoradiography using X-ray film. β-actin was detected on the same membrane and used as a loading control. Protein bands ($p34^{CDC2}$ and p-$p34^{CDC2}$ after 1, 4 or 24 h treatment) were quantified with the image analysis software Image J. Results were presented as normalized fold changes in relation to control. Normalization has been done using β-actin as a loading control.

2.7. Fluorescent microscopy

F-actin detection was performed on cells grown on coverslips and placed into a six-well plate. Cells were treated with the cucurbitacin glucoside combination (20 μM) in RPMI-1640 media for 4 or 24 h. Cells were fixed by 4% (w/v) PFA in PBS for 15 min at room temperature, washed in PBS, and permeabilized with 0.5% (v/v) Triton X-100 for 30 min at RT. Cells were washed three times in PBS and incubated with TRITC-labeled-phalloidin (P1951, Sigma) for 40 min in the dark. Preparations were washed and stained with Hoechst for 5 min, washed again in PBS and finally mounted in mounting medium 80% glycerol in PBS, 1% *n*-propyl gallate (Sigma). Microscopic observations were performed and photographed using a fluorescence microscope (Axiovert 200M) equipped with a HBO 100 W mercury lamp.

2.8. Annexin V/PI flow cytometric staining technique

Apoptosis was determined based on morphological change. Apoptotic cells were quantified by Annexin V-FITC and PI double-staining by using a staining kit purchased from MBL Co. Ltd. (Watertown, MA, USA).

2.9. JC-1 mitochondrial membrane potential detection assay

We used JC-1 (Sigma, MO, USA) for *in-situ* detection of mitochondrial membrane transition events in live cells, which provides an early indication of the initiation of cellular apoptosis. The collapse in the electrochemical gradient across the mitochondrial membrane ($\Delta\Psi$) was measured using a fluorescent cationic dye 5,5′,6,6′-tetrachloro-1,1′,3,3′-tetraethyl-benzamidazolocarbocyanin iodide, known as JC-1. In non-apoptotic cells, JC-1 exists as a monomer in the cytosol (green) and also accumulates as aggregates in the mitochondria (red). In apoptotic and necrotic cells, JC-1 exists in monomeric form and stains the cytosol green. For this assay, cells were treated with the cucurbitacin glucoside combination (0, 8, and 20 μM) and maintained at 37 °C in a humidified 5% CO_2 atmosphere for 24 h. Cells were washed with PBS and spun at 300 × *g*. The pellet was resuspended in 500 μl PBS, and 2 μl of 1 mg/ml JC-1 reagent was added for 20 min in 37 °C in the dark. Cells were washed with PBS and analyzed using a flow cytometer. Analysis was performed using Cell Quest software (BD Biosciences, San Jose, CA, USA) for apoptosis.

2.10. Statistical analysis

All experiments were performed at least three times. Where appropriate, the data are expressed as the mean ± standard error of the mean (S.E.M.). Probability (*P*) was calculated using a Student *t*-test. *P*-values lower than 0.05 were considered significant.

3. Results

3.1. Spectroscopic identification of isolated fraction

Fractions were isolated from the water extract of *C. colocynthis* leaves using TLC as described in Section 2, and their structure was determined by NMR spectroscopy (see Supplementary data). The fractions isolated are glycosylated cucurbitacin B and E (Fig. 1).

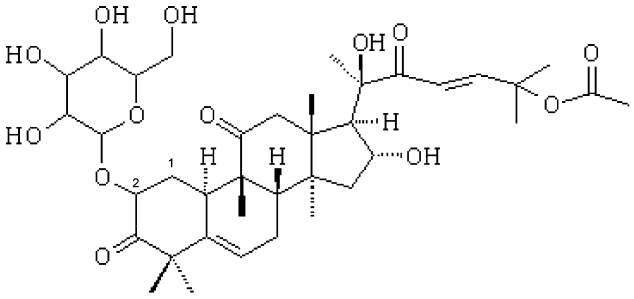

Fig. 1 – Chemical structure of cucurbitacin B glucoside (MW = 739). Structure of cucurbitacin E glucoside (MW = 737) is the same as cucurbitacin B glucoside except for a double bond between carbons 1 and 2.

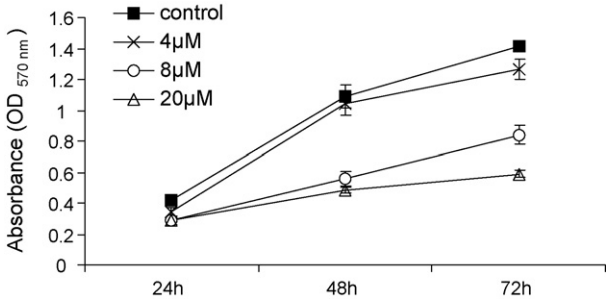

Fig. 2 – Dose-dependent effect of cucurbitacin glucoside combination (B and E in 1:1 ratio) on MDA-MB-231 proliferation. MDA-MB-231 cells at 7×10^3 cells/well were cultured with cucurbitacin glucoside combination (4, 8, and 20 μM) in RPMI-10% FCS. Daily cell proliferation was determined by MTT assay. The data represent the mean ± S.E. of three independent experiments. Effect of cucurbitacin glucoside combination is statistically significant in comparison with control ($P < 0.05$).

3.2. *Effect of cucurbitacin B and E glucoside combination on MCF-7 and MDA-MB-231 cell proliferation*

To evaluate the effect of cucurbitacin glucosides on cell proliferation of human breast cancer cell lines MCF-7 and MDA-MB-231, we initially treated both cell lines with escalating doses of the cucurbitacin glucoside combination (1:1). Cell proliferation was estimated by the MTT assay (as described in Section 2). The effect at various concentrations was studied after 24, 48, and 72 h of cell growth. Fig. 2 demonstrates that the cucurbitacin glucoside combination inhibited cellular proliferation in a dose-dependent manner. The proliferation of MDA-MB-231 cells was reduced by 50% upon a 48-h exposure to 8 μM cucurbitacin glucoside combination. Treating MCF-7 cells with cucurbitacin glucoside combination also inhibited cellular proliferation (data not shown). Antiproliferative activity of the cucurbitacin glucoside combination was further confirmed by counting live cells (using trypan blue exclusion dye). Proliferation of MDA-MB-231 cells was inhibited upon treatment in dose- and time-dependent manner (data not shown).

3.3. *Effect of cucurbitacin B/E glucosides and their combination on cell cycle*

To gain insights into the mechanism by which cell reduction is achieved, we investigated the effect on cell cycle distribution by fluorescence-activated cell sorting (FACS) analysis, and the results are summarized in Figs. 3 and 4. A 24-h exposure of MDA-MB-231 and MCF-7 cells to 20 μM cucurbitacin B glucoside or 25 μM cucurbitacin E glucoside caused ~3-fold enrichment of cells in G_2/M phase (Fig. 3). Exposure of MCF-7 cells to 20 μM of the cucurbitacin glucoside combination (1:1) also resulted in the accumulation of cells in the G_2/M phase. G_2/M enrichment was accompanied by a reduction in S phase cells, from 55% cells in the control to 3% cells following treatment (Fig. 4A). A histogram representing this G_2/M arrest is shown in Fig. 4B. In the following experiments, we used the combination of B and E cucurbitacin glucosides (1:1) since their

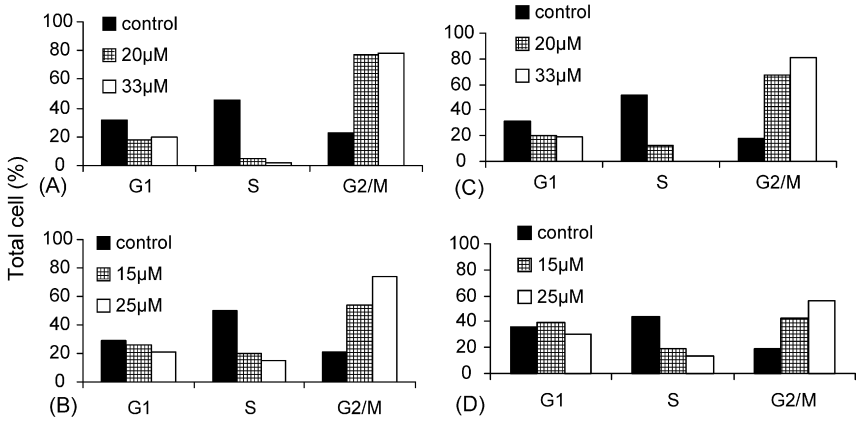

Fig. 3 – Effect of cucurbitacin B/E glucoside on cell-cycle distribution in MDA-MB-231 and MCF7 cells: (A) MDA-MB-231 cells treated with cucurbitacin B glucoside; (B) MDA-MB-231 cells treated with cucurbitacin E glucoside; (C) MCF-7 cells treated with cucurbitacin B glucoside; (D) MCF-7 cells treated with cucurbitacin E glucoside. The cells (5×10^5) were treated with cucurbitacin glucoside and analyzed at 24 h by DNA flow cytometry. Values indicate the percentage of cells in the indicated phases of the cell cycle. The data shown are representative of three independent experiments with similar findings.

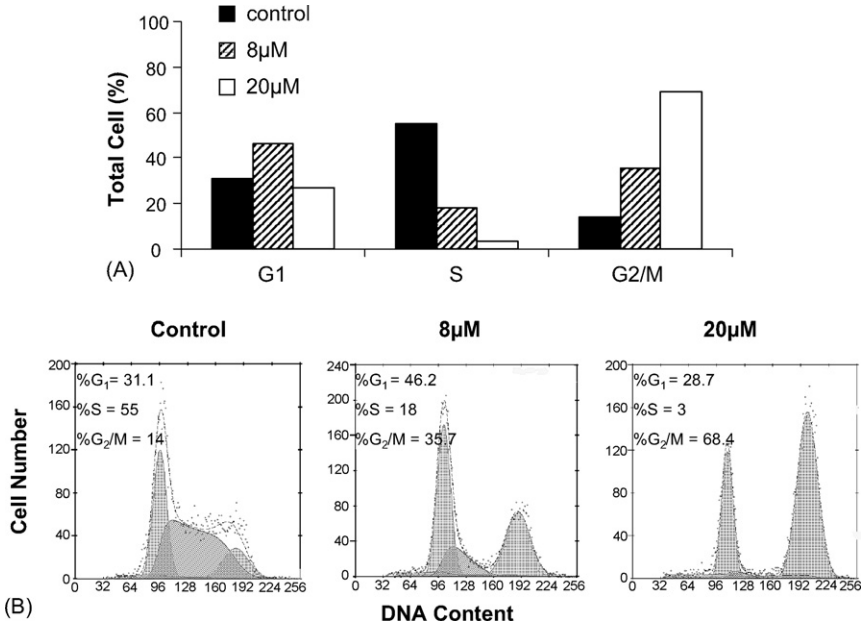

Fig. 4 – Effect of cucurbitacin glucoside combination (E + B) on cell-cycle distribution. (A) MCF7 cells treated with cucurbitacin glucoside combination (8 and 20 μM). The values indicate the percentage of cells in the indicated phases of the cell cycle. The data shown are representative of three independent experiments with similar findings. (B) Histograms show number of cells per channel (vertical axis) vs. DNA content (horizontal axis). MCF7 cells (5×10^5) were treated with 8 and 20 μM of cucurbitacin glucoside combination and analyzed at 24 h by DNA flow cytometry.

effect on cell cycle distribution was similar to the effect of each individual cucurbitacin glucoside (B/E).

3.4. *Effect of cucurbitacin glucoside combination on $p34^{CDC}$ and cyclin B1 expression*

In an attempt to understand the effect of the molecular events involved in cucurbitacin glucoside activity on cell cycle progression, we next investigated the effect of the cucurbitacin glucoside combination on the expression of proteins that are pivotal for G_2/M transition, including $p34^{CDC2}$ and cyclin B1. G_2/M transition requires activity of cyclin-dependent kinase, $p34^{CDC2}$. $p34^{CDC2}$ is positively regulated by association with cyclin B1 and negatively regulated by phosphorylation of amino acids Thr14 and Tyr15. Fig. 5A represents a typical Western blot from treated (20 μM cucurbitacin glucoside combination) and untreated cells. A decrease in the level of cyclin B1 and in the level of $p34^{CDC2}$ protein was observed at 24 h post-treatment. In many cases, especially those elicited by DNA damage agents, reduction in $p34^{CDC2}$ expression is preceded by $p34^{CDC2}$ phosphorylation at the inhibitory positions Thr14 and Tyr15. In order to find out if cucurbitacin glucoside combination treatment induces inhibitory phosphorylation of $p34^{CDC2}$, we followed the Thr14 and Tyr15 phosphorylation status of $p34^{CDC2}$ at early time points. As can be seen in Fig. 5B, a reduction in phospho-$p34^{CDC2}$ was observed as early as 1 h post-treatment. It seems that the cucurbitacin glucoside combination causes rapid elimination of $p34^{CDC2}$ protein, which is responsible for blocking G_2 to M transition. The mechanism by which this phenomenon occurs is not yet known but it is the focus of our present investigation. These results suggest that changes in expression of G_2/M regulating proteins may contribute to cucurbitacin glucoside-mediated cell-cycle arrest in MCF-7 and MDA-MB-231 cells.

3.5. *Effect of cucurbitacin glucoside combination on cell morphology and actin organization*

As previously described in the literature, cucurbitacin E was shown to interfere with cell cytoskeleton by causing marked disruption of the actin cytoskeleton [15,16]. In order to verify if the cucurbitacin glucoside combination had an effect on cell morphology, especially on cytoskeleton elements, we used light microscopy and performed staining analysis. Viewing cells after treatment (20 μM) compared to control, using light microscopy, clearly showed a deep change in the overall morphology of both MCF-7 and MDA-MB-231 cells from their typical morphology to round-shaped cells (Fig. 6). Interestingly, this effect on cell morphology appeared 1 h post-treatment (data not shown). Changes in cell shape are associated with reorganization of actin filaments [20], therefore, we examined the effect of cucurbitacin glucosides on actin distribution. Cells were stained with TRITC-labeled-phalloidin, which binds selectively to F-actin. As seen in Fig. 7, shortly after treatment (4 h), and 24 h later on, we observed changes in F-actin distribution from organized actin filament network underneath cell membrane and at the edges of control cells to accumulation of F-actin in the cytoplasm next to the nucleus, in cucurbitacin glucoside-treated cells. This effect was probably not a result of an apoptotic process, which is also characterized by round-cell

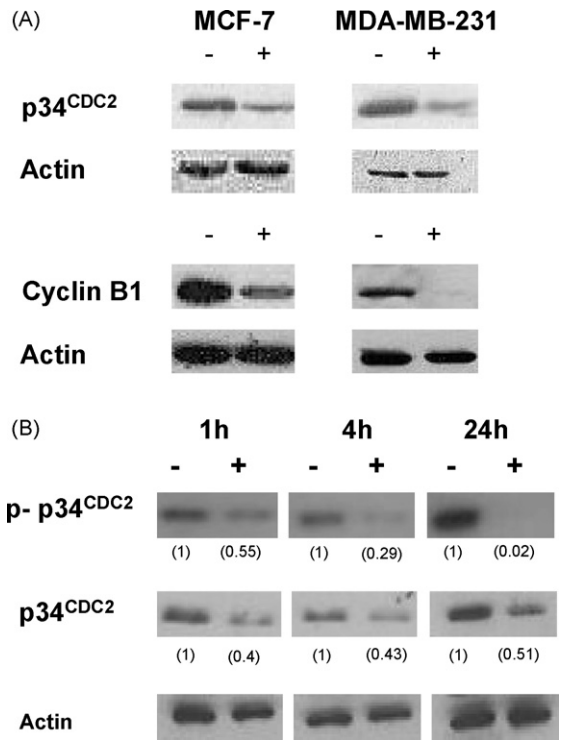

Fig. 5 – Western blot analysis of extracts obtained from MCF7 and MDA-MB-231 cells treated with the cucurbitacin glucoside combination. (A) Cells were treated with 0 (−) and 20 μM (+) cucurbitacin glucoside combination for 24 h. Extracts were prepared and analyzed by Western blotting with an antibody to p34^{CDC2} and cyclin B1. (B) MDA-MB-231 cells were treated with 0 (−) and 20 μM (+) cucurbitacin glucoside combination for 1, 4, and 24 h. Extracts were prepared and analyzed by Western blotting with an antibody to p34^{CDC2} and phospho-p34^{CDC2}. An antibody to β-actin was used as a loading control. Western blots are representative of three independent experiments. Quantification of the bands was performed and normalized change folds in relation to non-treated cells are shown in parenthesis. Normalization has been done using β-actin as a loading control.

morphology, since it appeared shortly after treatment when there was no evidence of cells undergoing apoptosis. Using a transmission electron microscope, we confirmed this actin reorganization. Control cells showed typical morphology while, in treated cells, the actin accumulated next to the nucleus (data not shown).

Lately, accumulating evidence in the literature indicates that cytoskeletal components are involved in downstream signal transduction pathways regulating cell survival [21]. For instance, it is reported that cytochalasin B, which causes cytoskeletal dearrangement [22], exhibits inhibition of proliferation, G_2/M arrest, and apoptosis. These effects closely resemble the effects of cucurbitacin glucosides, therefore, we hypothesize that cucurbitacin glucosides mediate their effects, at least partially, by altering cytoskeleton network, causing changes in cell morphology, which lead to both G_2/M arrest and apoptosis.

3.6. *Effect of cucurbitacin glucosides on STAT3 activity and signaling*

Recently, a study was published which demonstrated that cucurbitacin I and Q can interfere with STAT3 signaling by specifically inhibiting STAT3 phosphorylation [13]. Therefore, we were interested to find out the effect of the cucurbitacin glucoside combination on STAT3 phosphorylation in our cell system. Unexpectedly, we found that the cucurbitacin glucoside combination enhances rather than decreases STAT3 phosphorylation. This effect was detected early after treatment (4 h), and remained after 24 h treatment as well (Fig. 8). Constitutive activation of STAT3 has been shown in many different tumors. This activation usually results in an anti-apoptotic effect and promotes cell proliferation [23]. The effect of cucurbitacin glucosides on STAT3 phosphorylation is, therefore, incompatible with our previous results showing decrease in cell proliferation. We found a partial explanation for this enigma in the literature by combining the data of two different recently published papers concerning both STAT3 signaling and the consequences of cytoskeleton disruption. First, STAT3 was found to exhibit inhibitory activity on cell proliferation by enhancing p21^{WAF} expression in a specific situation in which both STAT3 activation and inhibition of PKB signaling occur simultaneously [24]. Another published study showed that disruption of actin cytoskeleton network reduces PKB signaling, culminating in reduction in the expression level of survivin (an IAP family member) which leads to both G_2/M arrest and apoptosis [22]. Since we observed both STAT3 activation and cell transition to round-cell morphology, which is a hallmark of cytoskeleton disruption, we suspected that cucurbitacin treatment brings about the specific condition in which STAT3 activity is exploited in favor of preventing cell proliferation rather than enhancing it. To verify this hypothesis, we looked at the key elements in this signaling scheme, namely p21^{WAF}, PKB, and survivin. Indeed, we can demonstrate that cucurbitacin glucoside treatment elevated p21^{WAF} expression, caused reduction in PKB phosphorylation, and, consequently, inhibited survivin expression, exactly as expected (Fig. 9A–C).

3.7. *Cucurbitacin glucoside combination induces apoptosis*

The apoptosis inducing effect of the cucurbitacin glucoside combination was evaluated by Annexin V/PI binding. One of the earliest events of apoptosis is the loss of plasma-membrane polarity, accompanied by translocation of phosphatidylserine (PS) from the inner to outer membrane leaflets, thereby exposing PS to the external environment [25]. The phospholipid-binding protein Annexin V has a high affinity for PS and can bind to cells with externally exposed PS. Positive staining with fluorescently labeled Annexin V correlates with loss of membrane polarity but precedes the complete loss of membrane integrity that accompanies the later stages of cell death resulting from either apoptosis or necrosis [25]. In contrast, PI can only enter cells after loss of membrane integrity. Thus, dual staining with Annexin V and PI allows clear discrimination between unaffected cells (Annexin V negative, PI negative), early apoptotic cells (Annexin V positive, PI negative), and late apoptotic cells (Annexin V positive, PI

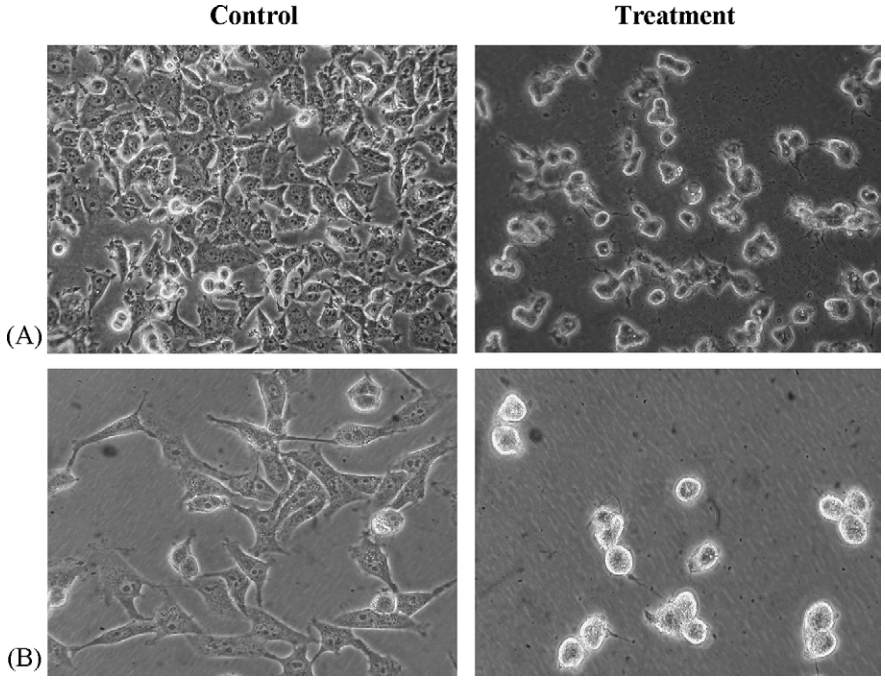

Fig. 6 – Effect of cucurbitacin glucosides combination treatment on (A) MCF-7 cell morphology and (B) MDA-MB-231 cell morphology. Cells were treated with 20 μM of the cucurbitacin glucoside combination (24 h) as indicated, and photographed (light microscopy, 20× magnification).

positive). As can be seen in Fig. 10, the cucurbitacin glucoside combination treatment (20 μM) increased the percentage of late apoptotic cells (presented in figure as UR) in MDA-MB-231 cells from 18.43% in control untreated cells to 61.35% in treated cells (Fig. 10A) (similar data were obtained for MCF-7 cells, data not shown). When the cucurbitacin glucoside combination was tested in two escalating concentrations (8 and 20 μM), induction of apoptosis showed dose dependency (Fig. 10B), which indicates that the apoptotic effect specifically resulted from the cucurbitacin glucoside treatment.

To further confirm our data, we used additional *in-situ* detection of apoptosis by measuring the effects of treatment on mitochondrial membrane potential ($\Delta\Psi$) using a fluorescent cationic dye 5,5′,6,6′-tetrachloro-1,1′,3,3′-tetraethylbenzamidazolocarbocyanin iodide, known as JC-1. In healthy cells, JC-1 exists as a monomer in the cytosol (FL1 positive; green) and also accumulates as aggregates in the mitochondria (FL2 positive; red). In apoptotic and necrotic cells, JC-1 exists exclusively in monomer form and produces a green cytosolic signal. As shown in Fig. 11, cucurbitacin glucoside combination treatment in MDA-MB-231 cells elevated the fraction of apoptotic cells from 11.17% in control cells to 48.58% in cells treated with 20 μM cucurbitacin glucoside combination. Herein we also observed dose response (Fig. 11).

4. Discussion

In the present study, we studied the inhibitory effect of cucurbitacin glucosides (B and E) isolated from *C. colocynthis* leaves, on breast cancer cells.

In these studies, the leaves of *C. colocynthis* were extracted with water, followed by a few more extractions (described in Section 2) to yield cucurbitacin B glucoside and cucurbitacin E glucoside purified fractions. Cucurbitacin B and E glucoside combination (1:1) exhibited growth inhibitory activity of human breast cancer cell lines in a dose- and time-dependent manner as can be seen by MTT assay (Fig. 2). Cucurbitacin B and E combination treatment inhibited cell growth with IC_{50} value of 8 μM for MDA-MB-231 cell line after 48 h. In order to elucidate the mechanism by which these extracts inhibited cell growth, we performed cell-cycle analysis. The cucurbitacin glucoside combination and each of the cucurbitacin glucosides alone induced cell-cycle arrest in the G_2/M phase of the cell cycle. Because of the similar effect on cell cycle distribution observed for each cucurbitacin glucoside alone or their combination, we decided to use a combination of the cucurbitacin glucosides in a 1:1 ratio for our subsequent experiments.

In order to get a better understanding of the mechanism by which the cucurbitacin combination leads to G_2/M arrest, we followed the status of key proteins known to regulate G_2/M transition, such as $p34^{CDC2}$ and cyclin B1. The $p34^{CDC2}$ protein kinase is generally acknowledged to be the key mediator of G_2/M phase transition in all eukaryotic cells [26]. The active mitotic kinase (MPF, or mitosis-promoting factor) is a dimer comprised of a catalytic subunit, a B-type cyclin, and a cyclin-dependent kinase termed $p34^{CDC2}$ or CDK1. The activity of the $p34^{CDC2}$ kinase not only depends on its association with cyclin B1, but also on its phosphorylation state. Phosphorylation of either Thr^{14} or Tyr^{15} inhibits $p34^{CDC2}$ kinase activity, while phosphorylation on Thr^{161} by CDK7 kinase is required for kinase activity. In addition, the dephosphorylation of Thr^{14} or Tyr^{15} by CDC25C phosphatase is a final step for $p34^{CDC2}$ kinase

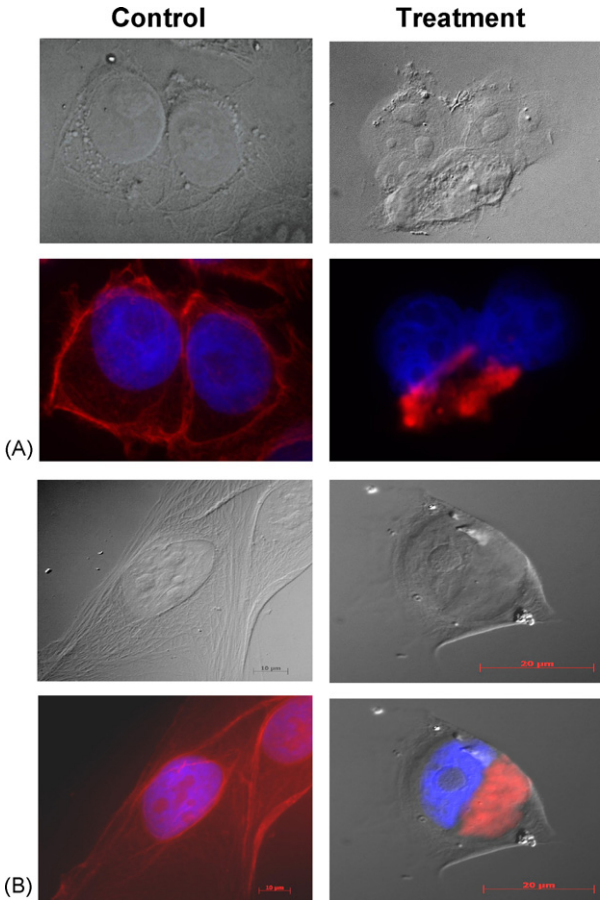

Fig. 7 – Effect of cucurbitacin glucoside combination (20 μM) on F-actin distribution in MDA-MB-231 cells, 4 h post-treatment (A) in MCF-7 cells, 24 h post-treatment (B). Cells were treated with cucurbitacin glucoside combination (20 μM), fixed and stained with TRITC-labeled-phalloidin and Hoechst and photographed (fluorescence microscope, 100× magnification). Upper photographs present DIC images, lower photographs present double-staining images (TRITC-labeled-phalloidin and Hoechst).

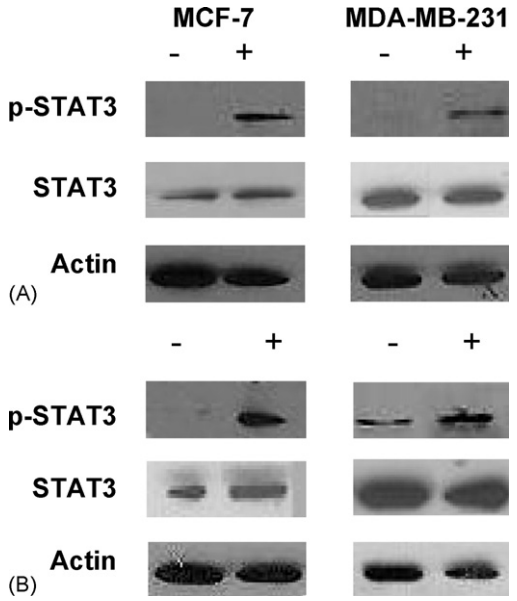

Fig. 8 – Effect of cucurbitacin glucoside combination on phospho-STAT3 expression. phospho-STAT3 expression was detected by Western blot analysis of extracts obtained from MCF7 and MDA-MB-231 cells treated with the cucurbitacin glucoside combination. Cells were treated with 0 (−) and 20 μM (+) cucurbitacin glucoside combination for 4 h (A) and 24 h (B). Extracts were prepared and analyzed by Western blotting with an antibody to STAT3 and phospho-STAT3 (Tyr 705). Antibody to β-actin was used as a loading control. Western blots are representative of three independent experiments.

activity [27,28]. We found that cucurbitacin glucoside treatment caused a reduction at the protein level of both $p34^{CDC2}$ and cyclin B1. The reduction of $p34^{CDC2}$ was very rapid and could be detected as early as 1 h post-treatment. By 24 h, only remnants of $p34^{CDC2}$ and cyclin B1 protein were observed (Fig. 5A). This phenomenon is even more impressive if we take into consideration that by 24 h of treatment, most of the cells were arrested in the G_2/M stage in which $p34^{CDC2}$ and cyclin B1 are mostly expressed. Moreover, when we followed phosphorylated $p34^{CDC2}$, we found a sharp decrease in phosphorylation status that followed a similar kinetics to the inhibition at the protein level (Fig. 5B). Thus, it is reasonable to hypothesize that cucurbitacin glucoside treatment causes cell cycle arrest at G_2/M by reducing the amount and, hence, the activity of $p34^{CDC2}$/cyclin B1 complex, which is necessary for G_2 to M transition, and not by inhibition of $p34^{CDC2}$ activity by its phosphorylation.

Recently, several studies were published pointing out that different cucurbitacin species exhibit various biological activities against tumor expansion. For instance, cucurbitacin I and Q were shown to specifically inhibit STAT3 phosphorylation which contributes to the proliferation of many cancerous cells [13,14]. In our study, we demonstrated a rapid and sustained elevation in the phosphorylated form of STAT3 (Fig. 8). This result was not compatible with the published data and at first seemed to be in contradiction to our own results concerning the antiproliferative effect of cucurbitacin glucosides treatment. This conflict was partially resolved when we considered the effects of cucurbitacin glucosides on cell morphology. We noticed a marked change in cell morphology, as was mentioned before in a study reporting that cucurbitacin E inhibits the proliferation of prostate cancer cells and causes disruption of the cytoskeleton structure of actin and vimentin [15,16]. cucurbitacin glucoside treatment caused disruption of the elongated shape of the cells toward a round-shaped appearance as was demonstrated by both light microscopy visualization (Fig. 6) and F-actin staining (Fig. 7). The F-actin network was shown to shift toward an accumulated form next to the nucleus instead of supporting cell shape by organization under the cell membrane. Two recently published articles revealed data that might connect between the multiple effects of cucurbitacin glucoside treatment. On one hand, disruption of actin cytoskeleton was shown to inhibit PKB phosphorylation and signaling, resulting in inhibition of

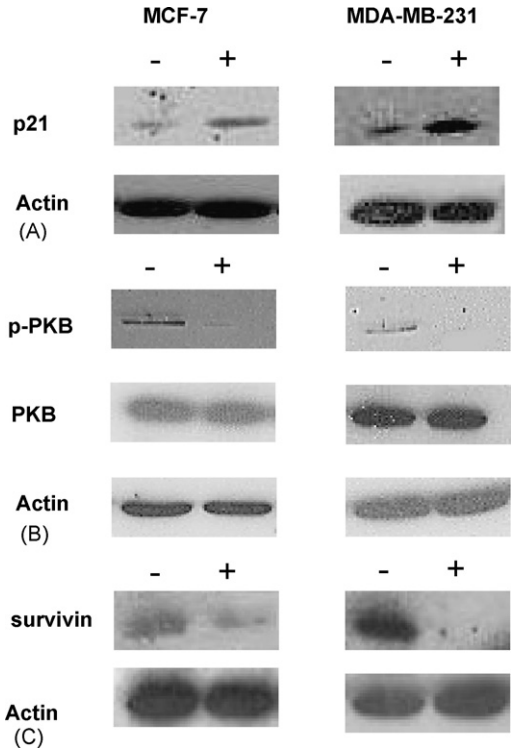

Fig. 9 – Western blot analysis of extracts obtained from MCF7 and MDA-MB-231 cells treated with the cucurbitacin glucoside combination. Cells were treated with 0 (−) and 20 μM (+) cucurbitacin glucoside combination for 24 h. Extracts were prepared and analyzed by Western blotting with an antibody to $p21^{WAF}$ (A); antibody to PKB and phospho-PKB (Ser 473) (B); antibody to survivin (C). Antibody to β-actin was used as a loading control. Western blots are representative of three independent experiments.

survivin expression [22], and on the other hand, another published paper reported that STAT3 activation can lead to $p21^{WAF}$ induction and, hence, inhibition of cell proliferation when STAT3 activation occurs concomitantly with PKB inhibition [24]. We speculate that these two occurrences explain the mechanism activated by cucurbitacin glucoside treatment, meaning that treatment causes both STAT3 activation (Fig. 8) and, at the same time, inhibits PKB phosphorylation through disruption of cytoskeleton filaments. As can be seen in Fig. 9, cucurbitacin glucoside treatment induced $p21^{WAF}$ expression as expected in a situation where STAT3 was enhanced in the presence of inhibited PKB phosphorylation. In addition, as expected from PKB dephosphorylation, we also detected a sharp reduction in survivin expression level (Fig. 9).

These results suggest that cucurbitacin glucoside treatment might have an even greater impact on tumor expansion than just G_2/M arrest and inhibition of cell proliferation since both survivin inhibition and discarding of actin filament can cause apoptotic cell death. Epithelial cells especially depend on their interaction with the extracellular matrix for survival [29], and the organization of actin filaments plays an important role in the formation of extracellular matrix connections [20,30,31]. Substances that inhibit cytoskeleton formation, such as okadaic acid, or cause actin depolymerization, such as cytochalasin B, were shown to induce apoptotic cell death, which involves changes in mitochondrial membrane potential [21,22,32]. Inhibition of survivin, which is a member of a family of proteins that inhibits apoptosis (IAP), can also contribute to induction of apoptosis, since survivin was shown to inhibit both activated caspases 9 and 3 [22]. The fact that cucurbitacin glucosides greatly inhibited survivin expression and disrupted actin polymerization implies that cucurbitacin glucosides might induce apoptosis. Therefore, we examined whether cucurbitacin treatment can induce apoptotic cell death by using two methods: cell-surface Annexin V binding, which measures the appearance of phosphatidylserine on the external plasma membrane, and JC-1 binding, which indicates changes in mitochondrial membrane potential [33,34]. Collapse of mitochondrial membrane potential is an accessory in the execution of apoptosis, which is directly dependent on cytoskeletal changes [21]. The two methods tested clearly showed (Figs. 10 and 11) an induction up to 3.5-fold in apoptotic cell fraction following cucurbitacin glucoside treatment. The differences in the percentage of apoptotic control cells between the methods used for apoptosis detection (Figs. 10 and 11), might partly reflect the difference in the sensitivity of the methods used.

As mentioned above, cucurbitacin glucoside treatment induced cell-cycle arrest in the G_2/M phase (68% of the cells) (Fig. 4) and, at the same time, displayed 60% cells in apoptosis (Fig. 10). These results might seem contradictory, but can be explained based on the fact that apoptotic cells are often accompanied by apoptotic body formation, which is reflected as sub-G_1 peak in FACS analysis. Since cucurbitacin glucosides interfere with actin cytoskeleton dynamics, which is a prerequisite for apoptotic body formation, no apoptotic bodies appear and therefore the apoptotic fraction is invisible by FACS analysis. The phenomenon of absence of apoptotic bodies was mentioned in the literature [32] regarding cytochalasin D, which is known to interfere with actin dynamics. Therefore, for apoptosis detection we used methods directed toward biochemical changes typical for cells in apoptosis, such as translocation of phosphatidyl serine from the inner to outer membrane leaflets (Fig. 10) and changes in mitochondrial membrane potential (Fig. 11). These methods reveal the apoptotic fraction that was unseen by FACS analysis. In other words, we suggest that at least part of the cells diagnosed as apoptotic cells are presented as cells in G_2/M phase using FACS analysis, since they still display 4N DNA content.

In conclusion, the results of the present study indicate that cucurbitacin glucosides effectively inhibited proliferation of both estrogen-dependent and estrogen-independent human breast cancer cells by causing G_2/M phase arrest and apoptosis. The mechanism by which cucurbitacin glucosides mediated this biological effect was partially revealed (Fig. 12). It is reasonable to hypothesize that cucurbitacin glucosides can be useful for chemotherapy of both estrogen-dependent and -independent breast cancers. A major issue concerning cucurbitacin therapeutic value is the overall toxicity of these compounds *in vivo*. The toxicity of *C. colocynhtis* fruits was tested on both rats and sheep by oral administration and

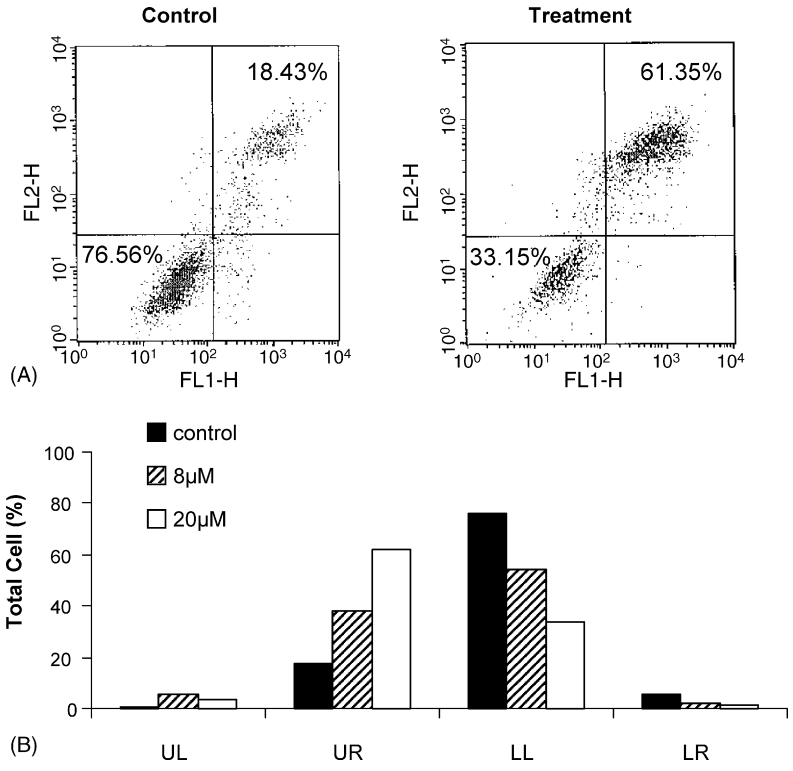

Fig. 10 – Annexin V binding and propidium iodide uptake induced by the cucurbitacin glucoside combination treatment: (A) MDA-MB-231 cells were treated with the cucurbitacin glucoside combination (20 μM) for 24 h, stained with Annexin V and propidium iodide, and analyzed by flow cytometry. The horizontal (FL1-H) and vertical (FL2-H) axes represent labeling with Annexin V and PI, respectively; (B) graphic presentation of data obtained by Annexin/PI staining after 24 h treatment using 8 and 20 μM cucurbitacin glucoside combination. UR represents late apoptotic cells (positive for both Annexin and PI), LL represents live cells. The data shown are representative of three independent experiments with similar findings.

although toxic effects were recorded, they were not fatal [11,35]. In a recently published study, a comparison between the cytotoxic effects of different cucurbitacin molecules was conducted and the final conclusion was that glycosylated molecules were less toxic than those that did not contain a glycoside moiety [36]. Since our cucurbitacin is glycosylated, we hope that therapeutic doses will not cause a fatal toxic effect and will be tolerable. Our future studies will focus on that issue to gain more information and deepened insight into the molecular targets of these molecules inside the cells in order to get a better comprehension of the way they induce cell-cycle arrest and apoptosis.

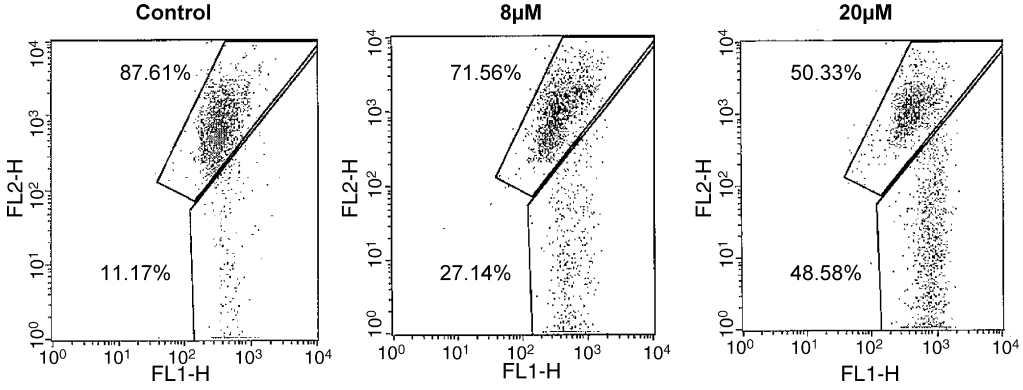

Fig. 11 – Effect of cucurbitacin glucoside combination on mitochondrial membrane potential. Cells were treated with cucurbitacin glucoside combination (8 and 20 μM) for 24 h to follow the extent of apoptosis by determination of mitochondrial membrane potential using JC-1 reagent. Cells were analyzed on a FACScan cytometer. Dot plots of red (FL2) vs. green fluorescence (FL1) show live cells with intact mitochondrial membrane potential and dead cells with lost mitochondrial potential, respectively. The data shown are representative of three independent experiments with similar findings.

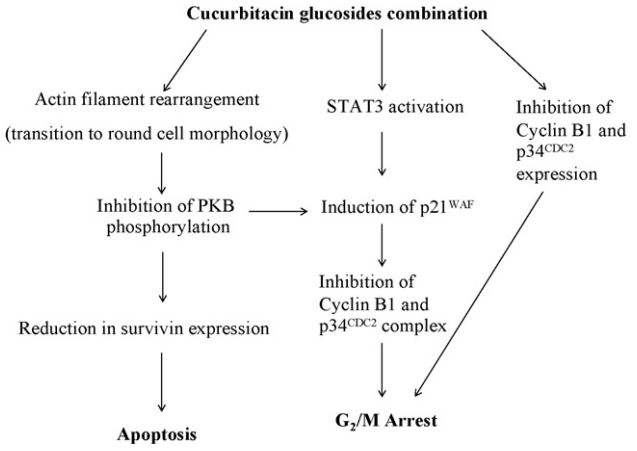

Fig. 12 – Proposed model for cucurbitacin glucoside-mediated G_2/M arrest and apoptosis. Following cucurbitacin glucoside treatment, dearrangement of actin filaments rapidly occurs, culminating in round-cell morphology. Dephosphorylation of PKB and activation of STAT3 were observed as well. This unique situation of simultaneous inhibition of PKB activity and STAT3 activation is possibly responsible for the observed induction in $p21^{WAF}$ expression. PKB inhibition might also lead to reduction in survivin, which promotes programmed cell death. Reduction in the protein level of key cell-cycle regulatory proteins such as $p34^{CDC2}$ and cyclin B1, was also detected. Taken together, these overall changes lead to both G_2/M arrest and apoptosis.

Acknowledgements

The authors would like to thank Prof. Zvi Malik and Ms. Judy Hanania for assistance with the use of the Transmission Electron Microscopy, and Mr. Uri Karo for assistance with the FACS. This research was partially supported by the Vinograd Foundation.

Appendix A. Supplementary data

Supplementary data associated with this article can be found, in the online version, at doi:10.1016/j.bcp.2006.09.012.

REFERENCES

[1] Chang JC. A review of breast cancer chemoprevention. Biomed Pharmacother 1998;52:133–6.
[2] Parker SL, Tong T, Bolden S, Wingo PA. Cancer statistics. CA Cancer J Clin 1997;47:5–27.
[3] Carolin KA, Pass HA. Prevention of breast cancer. Crit Rev Oncol Hematol 2000;33:221–38.
[4] Sporn MB, Suh N. Chemoprevention of cancer. Carcinogenesis 2000;21:525–30.
[5] Bergman M, Varshavsky L, Gottlieb HE, Grossman S. The antioxidant activity of aqueous spinach extract: chemical identification of active fractions. Phytochemistry 2001;58:143–52.
[6] Bergman M, Perelman A, Dubinsky Z, Grossman S. Scavenging of reactive oxygen species by a novel glucurinated flavonoid antioxidant isolated and purified from spinach. Phytochemistry 2003;62:753–62.
[7] Bakshi S, Bergman M, Dovrat S, Grossman S. Unique natural antioxidants (NAOs) and derived purified components inhibit cell cycle progression by downregulation of ppRb and E2F in human PC3 prostate cancer cells. FEBS Lett 2004;573:31–7.
[8] Lomnitski L, Bergman M, Nyska A, Ben-Shaul V, Grossman S. Composition, efficacy, and safety of spinach extracts. Nutr Cancer 2003;46:222–31.
[9] Tam NN, Nyska A, Maronpot RR, Kissling G, Lomnitski L, Suttie A, et al. Differential attenuation of oxidative/nitrosative injuries in early prostatic neoplastic lesions in TRAMP mice by dietary antioxidants. Prostate 2006;66:57–69.
[10] Breitbart E, Lomnitski L, Nyska A, Malik Z, Bergman M, Sofer Y, et al. Effects of water-soluble antioxidant from spinach, NAO, on doxorubicin-induced heart injury. Hum Exp Toxicol 2001;20:337–45.
[11] Adam SE, Al Yahya MA, Al Farhan AH. Response of Najdi sheep to oral administration of *Citrullus colocynthis* fruits, *Nerium oleander* leaves or their mixture. Small Rumin Res 2001;40:239–44.
[12] Jayaprakasam B, Seeram NP, Nair MG. Anticancer and antiinflammatory activities of cucurbitacins from *Cucurbita andreana*. Cancer Lett 2003;189:11–6.
[13] Blaskovich MA, Sun J, Cantor A, Turkson J, Jove R, Sebti SM. Discovery of JSI-124 (cucurbitacin I), a selective Janus kinase/signal transducer and activator of transcription 3 signaling pathway inhibitor with potent antitumor activity against human and murine cancer cells in mice. Cancer Res 2003;63:1270–9.
[14] Sun J, Blaskovich MA, Jove R, Livingston SK, Coppola D, Sebti SM, et al. Cucurbitacin Q: a selective STAT3 activation inhibitor with potent antitumor activity. Oncogene 2005;24:3236–45.
[15] Duncan KL, Duncan MD, Alley MC, Sausville EA. Cucurbitacin E-induced disruption of the actin and vimentin cytoskeleton in prostate carcinoma cells. Biochem Pharmacol 1996;52:1553–60.
[16] Duncan MD, Duncan KL. Cucurbitacin E targets proliferating endothelia. J Surg Res 1997;69:55–60.
[17] Peters RR, Saleh TF, Lora M, Patry C, de Brum-Fernandes AJ, Farias MR, et al. Anti-inflammatory effects of the products from *Wilbrandia ebracteata* on carrageenan-induced pleurisy in mice. Life Sci 1999;64:2429–37.
[18] Yesilada E, Tanaka S, Sezik E, Tabata M. Isolation of an anti-inflammatory principle from the fruit juice of *Ecballium elaterium*. J Nat Prod 1988;51:504–8.
[19] Mosmann T. Rapid colorimetric assay for cellular growth and survival: application to proliferation and cytotoxicity assays. J Immunol Meth 1983;65:55–63.
[20] Burridge K, Chrzanowska-Wodnicka M. Focal adhesions, contractility, and signaling. Annu Rev Cell Dev Biol 1996;12:463–518.
[21] Cabado AG, Leira F, Vieytes MR, Vieites JM, Botana LM. Cytoskeletal disruption is the key factor that triggers apoptosis in okadaic acid-treated neuroblastoma cells. Arch Toxicol 2004;78:74–85.
[22] Liang YL, Wang LY, Wu H, Ma DZ, Xu Z, Zha XL. PKB phosphorylation and survivin expression are cooperatively regulated by disruption of microfilament cytoskeleton. Mol Cell Biochem 2003;254:257–63.
[23] Yu H, Jove R. The STATs of cancer: new molecular targets come of age. Nat Rev Cancer 2004;4:97–105.
[24] Barré B, Avril S, Coqueret O. Opposite regulation of Myc and $p21^{WAF1}$ transcription by STAT3 proteins. J Biol Chem 2003;278:2990–6.

[25] Vermes I, Haanen C, Steffens-Nakken H, Reutelingsperger C. A novel assay for apoptosis. Flow cytometric detection of phosphatidylserine expression on early apoptotic cells using fluorescein labelled Annexin V. J Immunol Meth 1995;184:39–51.
[26] Liang YC, Tsai SH, Chen L, Lin-Shiau SY, Lin JK. Resveratrol-G2 arrest through the inhibition of CDK7 and $p34^{CDC2}$ kinases in colon carcinoma HT29 cells. Biochem Pharmacol 2003;65:1053–60.
[27] Molinari M. Cell cycle checkpoints and their inactivation in human cancer. Cell Prolif 2000;33:261–74.
[28] Hartwell LH, Kastan MB. Cell cycle control and cancer. Science 1994;266:1821–8.
[29] Martin SS, Leder P. Human MCF10A mammary epithelial cells undergo apoptosis following actin depolymerization that is independent of attachment and rescued by Bcl-2. Mol Cell Biol 2001;21:6529–36.
[30] Maniotis AJ, Chen CS, Ingber DE. Demonstration of mechanical connections between integrins, cytoskeletal filaments, and nucleoplasm that stabilize nuclear structure. Proc Natl Acad Sci USA 1997;94:849–54.
[31] Parsons JT, Martin KH, Slack JK, Taylor JM, Weed SA. Focal adhesion kinase: a regulator of focal adhesion dynamics and cell movement. Oncogene 2000;19:5606–13.
[32] Yamazaki Y, Tsuruga M, Zhou D, Fujita Y, Shang X, Dang Y, et al. Cytoskeletal disruption accelerates caspase-3 activation and alters the intracellular membrane reorganization in DNA damage-induced apoptosis. Exp Cell Res 2000;259:64–78.
[33] Bijl M, Horst G, Bijzet J, Bootsma H, Limburg PC, Kallenberg CG. Serum amyloid P component binds to late apoptotic cells and mediates their uptake by monocyte-derived macrophages. Arthritis Rheum 2003;48: 248–54.
[34] Nihal M, Ahmad N, Mukhtar H, Wood GS. Anti-proliferative and proapoptotic effects of (−)-epigallocatechin-3-gallate on human melanoma: possible implications for the chemoprevention of melanoma. Int J Cancer 2005;114: 513–21.
[35] Al Yahya MA, Al Farhan AH, Adam SE. Preliminary toxicity study on the individual and combined effects of *Citrullus colocynthis* and *Nerium oleander* in rats. Fitoterapia 2000;71:385–91.
[36] Bartalis J, Halaweish FT. Relationship between cucurbitacins reversed-phase high-performance liquid chromatography hydrophobicity index and basal cytotoxicity on HepG2 cells. J Chromatogr B Anal Technol Biomed Life Sci 2005;818:159–66.